

IDENTIFICATION OF THE NEAR-WALL FLOW STRUCTURES RESPONSIBLE FOR THE LARGE INSTANTANEOUS DEVIATIONS OF THE MOMENTUM AND HEAT TRANSFER ANALOGY IN A FULLY DEVELOPED TURBULENT CHANNEL FLOW

J. Pallares, A. Vernet, J. A. Ferré and F. X. Grau

Department of Mechanical Engineering, University Rovira i Virgili

Av. Països Catalans, 26. 43007-Tarragona, Spain

pallares@etseq.urv.es, avernet@etseq.urv.es, jafferre@etseq.urv.es, xgrau@etseq.urv.es

ABSTRACT

In this paper we analyze the spatial distribution of the instantaneous departures from the conventional analogy between momentum and heat transfer of a pressure driven fully developed turbulent channel flow at low Reynolds numbers ($Re=4570$, $Pr=0.7$). The analysis was carried out using a database obtained from a direct numerical simulation performed with a second-order finite volume code. The ensemble averaged velocity and temperature profiles and profiles of the turbulence intensities and turbulent heat fluxes agree well with direct numerical simulations available in the literature. When the flow was statistically fully developed, we recorded the time evolution of the velocities and temperatures near one wall of the channel. The near wall structures responsible for the extreme values of the deviations were deduced by a conditional sampling technique. Results show that extreme values of the departures from the analogy occur within the imprints of the high-speed streaks on the wall and are associated with large positive fluctuations of the wall shear stress and wall heat flux. These large fluctuations on the wall are produced by the combined effect of two quasi-parallel counterrotating streamwise vortices.

INTRODUCTION

The analysis of the relationship between the wall shear stress in bounded turbulent flows and the near wall flow structures has been received considerable attention to better understand the generation and the dynamics of the substantial increase of skin friction generated by turbulent boundary layers in comparison with the laminar ones (Kim et al., 1987; Kravchenko et al. 1993). Experimental measurements and analysis of the databases of numerical simulations of fully developed turbulent channel flows have shown that the near wall region is populated by quasi-streamwise vortices that are convected along the axial direction by the flow. These streamwise vortices

coexist with the streaky structure of the near wall region that consists in unsteady axially elongated streaks of high speed and low speed flow that are alternated along the spanwise direction (Jeong et al. 1997).

The typical topology of the quasi-streamwise vortices has been obtained and described by applying conditional sampling techniques in databases of numerical simulations of channel flows (Matsubara et al., 2001). Recently, their effect on the fluctuations of the wall heat flux has been reported by Abe et al. (2004) and the similarity of these fluctuations to the fluctuations of the wall shear stress demonstrated. This similarity suggests the possibility to infer the local instantaneous wall shear stress from the local instantaneous wall heat flux, or viceversa.

We selected the conventional Reynolds analogy (Eq. 1) as the starting point to analyze the properties of this instantaneous similarity.

$$\frac{Cf}{2} = \frac{Nu}{RePr^{1/3}} \quad (0.6 < Pr < 60) \quad (1)$$

Equation 1 relates fairly well the values of the averaged friction coefficient, $\langle Cf \rangle$, and Nusselt number, $\langle Nu \rangle$, in fully developed turbulent channel flows because on average the near wall flow conditions are insensitive to the effect of the pressure gradient. In fact, the differences in the averaged velocity and temperature profiles for different boundary layers subjected to different averaged pressure gradients are found far from the wall, in the logarithmic and wake regions of the profiles. On the other hand, it is known that Eq. 1 is not adequate to relate the instantaneous values of Cf and Nu because of the important contribution of the fluctuating pressure gradient to the instantaneous streamwise momentum budget on the wall invalidates the analogy. However the analysis of the

instantaneous deviations of the analogy and their relation with the quasi-streamwise vortices can be useful to develop an effective procedure to determine the local instantaneous wall shear stress, for example, from the measurement of the local instantaneous wall heat flux. This procedure would be particularly valuable for flow control techniques oriented to the reduction of drag in turbulent flows.

MODEL

Figure 1 shows the coordinate system and the computational domain of the plane channel. The forced convection incompressible flow, driven by an externally imposed mean pressure gradient, is assumed to be hydrodynamically and thermally fully developed. The two walls of the channel ($y=-L_y/2$ $y=L_y/2$) are rigid, smooth and heated with a constant and uniformly distributed heat flux (q''_w) along the axial direction with constant peripheral wall temperature. All physical properties of the fluid, with a Prandtl number ($Pr=\nu/\alpha$) of 0.7, are considered constant with the temperature. Viscous dissipation and radiation heat transfer are neglected.

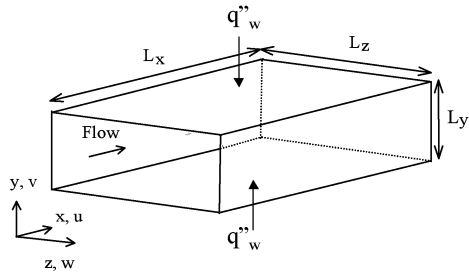


Figure 1. Physical model and coordinate system

The non-dimensional continuity, Navier-Stokes and thermal energy equations are

$$\frac{\partial u_i}{\partial x_i} = 0 \quad (2)$$

$$\frac{\partial u_i}{\partial t} + \frac{\partial u_j u_i}{\partial x_j} = \delta_{ij} - \frac{\partial p}{\partial x_i} + \frac{1}{Re_\tau} \frac{\partial^2 u_i}{\partial x_j \partial x_j} \quad (3)$$

$$\frac{\partial \theta}{\partial t} + \frac{\partial u_j \theta}{\partial x_j} = \frac{u_1}{U_b} + \frac{1}{Pr Re_\tau} \frac{\partial^2 \theta}{\partial x_j \partial x_j} \quad (4)$$

respectively.

The scales used to obtain the non-dimensional variables are the channel half-width ($D=L_y/2$) and the average friction velocity ($u_\tau^2=\tau_w/\rho$). The non-dimensional

temperature is defined as $\theta = ((T_w) - T) \rho C_p u_\tau / q''_w$ where $\langle T_w \rangle$ is the wall temperature which only depends on x and increases linearly along the streamwise direction according to the fully developed flow hypothesis. Pressure is scaled with the average wall stress (τ_w). In Eq. (3), δ_{ij} is the averaged non-dimensional pressure gradient along the x -direction, which is assumed to be constant. The second term on the right-hand side of Eq. (4) arises from the decomposition of the instantaneous temperature field in a streamwise periodic contribution (θ) and a linear dependent contribution along the x direction. This term corresponds to the dimensional term, $-u \, d\langle T_w \rangle / dx$. In Eq. (4) Re_τ is the Reynolds number ($Re_\tau = u_\tau D / \nu = 150$) and U_b is the non-dimensional bulk velocity ($U_b = U / u_\tau$).

The computational domain, with dimensions $L_x=12.6$, $L_y=2$, $L_z=3.1$, is divided into $121 \times 100 \times 121$ grid nodes. They are uniformly distributed along the streamwise and spanwise homogeneous directions ($\Delta x^+ \approx 15.8$ and $\Delta z^+ \approx 4$) in which periodic boundary conditions are imposed, while hyperbolic tangent distributions are used to stretch the nodes near the walls where the no-slip condition is applied. For the Reynolds number considered ($Re = U_2 D / \nu = 4570$), the minimum and maximum grid spacing in the directions perpendicular to the walls are $(\Delta y^+)_{\min} \approx 0.5$ and $(\Delta y^+)_{\max} \approx 6.6$. A constant wall temperature in terms of the non-dimensional temperature (i.e. $\theta_w = 0$) is imposed at the channel walls.

The governing transport equations, Eqs. (2 to 4), are solved numerically with the 3DINAMICS code. This second-order accuracy finite volume code uses central differencing of the diffusive and convective terms on a staggered grid and a Crank-Nicolson scheme for the temporal discretization. More details about the code can be found in Pallares et al. (2002)

RESULTS AND DISCUSSION

We recorded the spatial distributions of the velocity and temperature fields near the bottom wall of the channel when the flow was statistically fully developed. The database generated contains the time evolution during 25 letots (5000 time steps) of the three components of the velocity vector, the pressure and the temperature in 50 y -planes of 121×121 grid nodes located at $-L_y/2 \leq y < 0$. The instantaneous wall shear stresses and heat fluxes were computed assuming a linear variation of velocities and temperatures within the distance between the first near wall grid node located at $y^+ = 0.5$ and the wall. The period of non-dimensional time recorded is about 50 times the integral time scale of the wall shear stress evolution. As a physical example, 25 letots correspond to 0.2 (3.2) seconds in an air (water) flow with an average velocity of 9.3 (0.6) m/s through a channel with $L_y = 1$ cm.

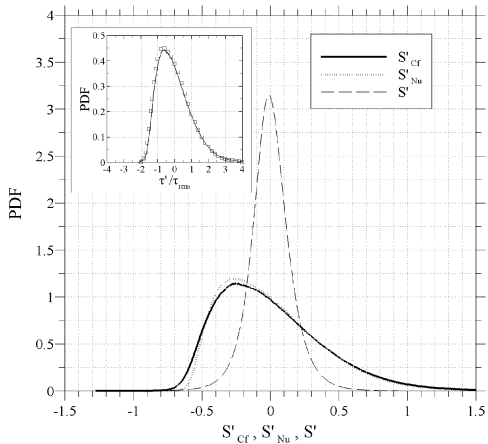


Figure 2. PDF of S'_{Cf} , S'_{Nu} and S' . The inset shows the comparison between the PDFs of the fluctuations of the wall shear stress predicted by DNS of Kim et al. (1987) (symbols) and by the present DNS (continuous line)

The conventional analogy between the instantaneous and local momentum and heat transfer rates in the range $0.6 < Pr < 60$, Eq. (1), can be rewritten as

$$S = \frac{Cf}{2} - \frac{Nu}{Re Pr^{1/3}} \quad (5)$$

$$S = \frac{\langle Nu \rangle}{Re Pr^{1/3}}$$

where $Cf = 2\mu (\partial u / \partial y|_w) / (\rho U^2)$ and $Nu = 2D h/k$ are the local instantaneous friction coefficient and the local instantaneous Nusselt number, respectively. In Eq. (5), $\langle Nu \rangle = 2D \langle h \rangle / k$ is the averaged Nusselt number and S is a parameter that measures the fractional instantaneous deviation from the analogy (i.e. $S=0$ if the analogy holds and $S=0.5$ if the value of $Cf/2$ is 50% over the value of $Nu/[Re Pr^{1/3}]$).

To analyze the dynamical properties of the deviations of the analogy, we define the instantaneous momentum (S_{Cf}) and heat (S_{Nu}) transfer contributions to the right-hand side of Eq. (5) as

$$S = S_{Cf} - S_{Nu}, \quad S_{Cf} = \frac{Cf Re Pr^{1/3}}{2 \langle Nu \rangle}, \quad S_{Nu} = \frac{Nu}{\langle Nu \rangle} \quad (5)$$

The quantities S_{Cf} and S_{Nu} can be interpreted as non-dimensional measures of the instantaneous main wall shear stress ($\partial u / \partial y|_w$) and wall heat flux. In our simulations the averaged values of $Cf=0.00863$ and $Nu=15.4$ agree with those reported by Kasagi et al. (1992) ($Cf=0.00858$, $Nu=15.4$) at the same Re_τ and using the same boundary conditions. The averaged value of the deviation parameter $\langle S \rangle = 0.13$ indicates that the analogy is only approximately valid at the low Reynolds number considered and the fluctuating intensities of S

($S'' = \langle S^2 \rangle^{1/2} / \langle S \rangle = 0.24$) suggest that the instantaneous deviations are significant. Irrespectively of the limited validity of the analogy, the analysis presented in this study is focused in the fluctuations of S_{Cf} , S_{Nu} and S (for example $S'_{Cf} = S_{Cf} - \langle S_{Cf} \rangle$).

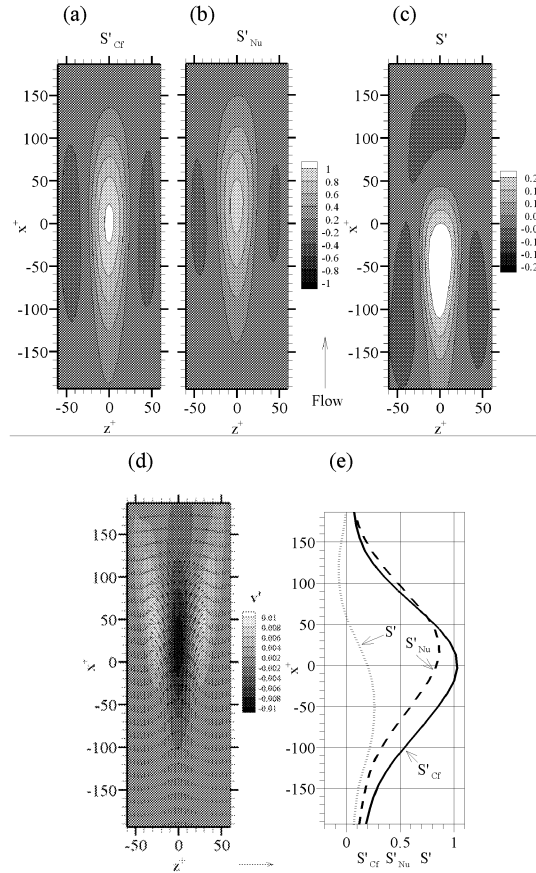


Figure 3. Conditional sampled imprints of the flow leading to extreme values of the deviation from the analogy. (a) ensemble averaged streamwise wall shear stress fluctuations in terms of S'_{Cf} ; (b) ensemble averaged wall heat flux in terms of S'_{Nu} ; (c) ensemble averaged S' ; (d) conditionally sampled velocity field as the vector plot of u' and w' superimposed to the contours of v' at $y^+=0.5$ (e) profiles of S'_{Cf} , S'_{Nu} and S' along the line $z^+=0$

Analysis of the imprints

Figure 2 shows the probability density functions (PDFs) of S'_{Cf} , S'_{Nu} and S' . It can be seen that the PDFs of S'_{Cf} and S'_{Nu} are nearly coincident and that the negative values of the fluctuations of S_{Cf} or S_{Nu} are about 60% more probable than positive values. It can be seen in Fig. 2 that the PDF of S' has a high degree of symmetry. The inset in Figure 2 shows that there is a good agreement between the PDF of the wall shear stress fluctuations predicted by DNS of Kim et al. (1987) and those of the present computation. The DNS data is taken from Naqwi and

Reynolds (1991) because the PDF is not reported in the original paper of Kim et al. (1987).

We applied a conditional pattern recognition technique to the streamwise velocity fluctuating component in the first near-wall plane of grid points which are located at $y^+=0.5$ to obtain an ensemble average of the typical footprints of the structures that are responsible for the extreme local deviations from the analogy. It should be noted that the local instantaneous friction factor and Nusselt number are proportional to the streamwise velocity component and temperature, respectively, in the first near-wall node if a linear variation of their instantaneous values is assumed within this distance from the wall. The extreme values of S' are generally associated with large values of the fluctuations of the streamwise shear stress (or fluctuations of the streamwise velocity component in the first near-wall node). For this reason, we used the fluctuations of the streamwise velocity component (u') to obtain the averaged imprint associated with the extreme deviations from the analogy.

The pattern recognition technique applied is based on the computation of the cross-correlation between an initial template and the instantaneous spatial two-dimensional distributions of u' for all the recorded time steps. The template used consists of a positive lobe of u' in a region with dimensions $\Delta x^+=600$ and $\Delta z^+=140$. The dimensions of the lobe and of the region were selected according to the characteristic streamwise and spanwise sizes of S' and C_f deduced by the autocorrelations, not shown here for sake of brevity.

The correlation coefficients are stored in a three-dimensional matrix (i.e. a two-dimensional matrix for each time step). The regions where local maxima of correlation occur conform volumes that are elongated in time, according to the fact that the time history of the extreme values of u' (or C_f') are convected along the streamwise direction. Within these volumes only the region (with dimensions $\Delta x^+=600$ and $\Delta z^+=140$) of the plane of time where the absolute maximum of correlation occur is selected for averaging. This procedure prevents the selection of the different stages of the same event at different times. A total of 2100 individual events were used to obtain the ensemble average of the imprints.

Figure 3.a shows the ensemble average of the fluctuations of S_{CF} . The information of the location in the database where the individuals used to compute this ensemble average was utilized to conditionally obtain the ensemble averages of, S_{Nu} (Fig. 3.b), S' (Fig. 3.c), and the velocity field u' , v' and w' at the first near wall plane of nodes (Fig. 3.d).

As expected, large positive fluctuations of the wall shear stress (Fig. 3.a) produce large fluctuations of the wall heat flux (Fig. 3.b). However the maximum value of the wall shear stress appears retarded with respect to the

maximum value of the wall heat flux by about $\Delta x^+=20$, as shown in the profiles of S'_{CF} , S'_{Nu} and S' along $z^+=0$, plotted in Fig. 3.e. The conditional averaged flow in the first near wall plane of grid nodes shows that the imprint of the streamwise current of high x -momentum fluid is accelerated towards the center of the template region ($x^+=0$, $z^+=0$) and then is diverted towards the spanwise direction. The contours of v' indicate that the maximum of u' is associated with a descending current towards the wall which is also centered at $x^+=0$, $z^+=0$, and that the diverted flow tends to leave the wall (i.e. v' positive). The effect of the impinging current in the region where the flow is diverted towards the z direction and thus the streamwise velocity u' is decreased produces the displacement of the maximum of the wall heat flux (Fig. 3.b) with respect to the maximum of the wall shear stress (Fig. 3.a). Accordingly, Figure 3.c shows that the fluctuations of the deviation parameter attain negative/positive values at the front/rear of the imprint. The averaged values of these maximum deviations are within ± 0.2 which is about the rms of the fluctuations of the deviation parameter S . (see for example the PDF of S' shown in Fig. 2). Inspection of instantaneous near wall flow fields and the crosscorrelations between the fluctuations of the streamwise pressure gradient at the wall and the fluctuations of S , not shown here for brevity, show that the extreme values of S' occur within the high speed streaks and have a with a characteristic spatial periodicity associated with fluctuations of the streamwise pressure gradient.

Near-wall flow structures

The convection velocity of the large fluctuations of u' (or C_f) computed as the streamwise displacement of the maximum correlation between two successive time steps divided by the time step is 10.1, in agreement with the value of 9.6 reported by Jeon et al. (1999) in their analysis of DNS data. This value suggests that the events or flow structures that produce large fluctuations of the wall shear stress occur, on average, at a distance from the wall of about $y^+\approx 10$.

To educe the near wall structures responsible for the large fluctuations of shear stress we averaged the flow above the wall for the events selected to obtain the conditional average imprint on the wall shown in Fig. 3. The flow topology is depicted in Fig. 4 in terms of three views of the isosurface of a negative value of the second invariant of the velocity gradient tensor (λ_2), a quantity proposed by Jeong et al. (1997) to detect the occurrence of vortex cores. Figures 4.s-1 to 4.s-3 correspond to the velocity field in the three planes indicated in Fig. 4.a. It can be seen in Figure 4 that the large positive fluctuation of the wall shear stress is located near the tail of a pair of counterrotating streamwise vortices which convect high momentum fluid towards the wall in the region between them. The vortices show an inclination of 8° in the xy plane and a tilting angle of $\pm 3^\circ$ in the xz plane in

agreement with Jeong et al. (1997) who reported 9° and $\pm 4^\circ$, respectively, in their conditional averaged flow based on the detection of individual streamwise vortices using the criterion of λ_2 . The similarity between the sizes and diameters of the vortices shown in Fig. 4 and those reported by Jeong et al. (1997) also suggest that the large fluctuations of the wall shear stress are associated with the same kind of structures detected by these authors.

To clarify if the structure responsible for the large positive fluctuations of the wall shear stress detected has simultaneously the two parallel streamwise vortices shown in Fig. 4 or, alternatively, the fluctuation can be produced by a single vortex that in some individuals appears at $z^+>0$ and in some others appears at $z^+<0$, we classified the individuals into three groups. The classification criterion adopted was the degree of correlation between the distribution of w of the imprint of each individual and three templates of w . As can be inferred from Fig. 3.d the distribution of w has one negative lobe at $z^+<0$ and one positive lobe at $z^+>0$. One of the templates of w consisted in the conditional sampled imprint with the two symmetrically distributed lobes with respect to $z^+=0$. The other two templates were constructed eliminating one of the lobes (i.e. one with only one positive lobe at $z^+>0$ and the other with one negative lobe at $z^+<0$). It was found that about 70% of the individual imprints have a high degree of correlation with the first template with the two lobes and the corresponding averaged flow structure shows two symmetrically distributed streamwise vortices. About half of the rest of the individuals (15%) were well correlated with the template with the positive lobe and the remaining 15% with the template with the negative lobe. The averaged flow structures associated with these non-symmetric imprints with respect to $z^+=0$ consist in one streamwise vortex with similar dimensions as that shown in Fig. 4, with its tail above the imprint, and accompanied by a much smaller vortex parallel to the main vortex. This analysis indicates that the large positive fluctuations of the wall shear stress, wall heat flux or the large deviations from the analogy have mainly associated the simultaneous effect of two parallel counterrotating streamwise vortices.

CONCLUSIONS

The conventional analogy between instantaneous momentum and heat transfer on a wall has been investigated using numerical results of a direct numerical simulation of a forced convection turbulent flow in a plane channel. Although the analogy holds for the averaged values of the friction factor and Nusselt number, it has been found that the imprints on the wall of the instantaneous streaky flow structure of the viscous sublayer produce significant deviations from the analogy. Locally and instantaneously the deviations can be of the order of 25%. The large deviations from the analogy occur within the imprints of the high-speed streaks. These streaks present spots of large positive fluctuations of the

main wall shear stress that appear spatially retarded with respect the corresponding fluctuations of the wall heat flux by about 25 wall units causing the large deviations from the analogy. The conditional averaged flow field responsible for these large deviations consists in the simultaneous occurrence of two parallel counterrotating vortices that convect high momentum fluid towards the wall and induce extreme values of the instantaneous wall shear stress and thus heat flux and deviation parameter near their tail.

ACKNOWLEDGMENTS

This study was financially supported by the Spanish Ministry of Science of Technology and FEDER under projects DPI2003-06725-C02-01 and VEM2003-20048.

REFERENCES

- Abe, H., Kawamura, H., Matsuo, Y., 2004, "Surface heat-flux fluctuations in a turbulent channel flow up to $Re=1020$ with $Pr=0.025$ and $Pr=0.71$," *International Journal of Heat and Fluid Flow*, Vol. 25, pp. 404-419
- Jeon, S., Choi, H., Yoo, J. Y., and Moin, P., 1999 "Space-time characteristics of the wall shear stress fluctuations in a low Reynolds-number channel flow", *Physics of Fluids*, Vol. 11, pp. 3084-3094
- Jeong, J., Hussain, F., Schoppa, W., and Kim, J., 1997, "Coherent structures near the wall in a turbulent channel flow", *Journal of Fluid Mechanics*, Vol. 332, pp. 185-214
- Kasagi, N., Tomita, Y., Kuroda, A., 1992, "Direct numerical simulation of passive scalar field in a turbulent channel flow," *ASME Journal of Heat Transfer*, Vol. 114, pp. 598-606
- Kim, J., Moin, P., Moser R., 1987, "Turbulence statistics in fully developed channel flow at low Reynolds number", *Journal of Fluid Mechanics*, Vol. 177, pp. 133-166
- Kravchenko, A. G., Choi, H., Moin, P., 1993, "On the relation of near-wall streamwise vortices to wall skin friction in turbulent boundary layers," *Physics of Fluids* Vol. 5, pp. 3307-3309
- Matsubara, K., Kobayashi, M., Sakai, T., Suto, H., 2001, "A study on spanwise heat transfer in a turbulent channel flow - eduction of coherent structures by a conditional sampling technique," *International Journal of Heat and Fluid Flow*, Vol. 22, pp. 213-219
- Naqwi, A. A., Reynolds, W. C., 1991, "Measurement of turbulent wall velocity gradients using cylindrical waves of laser light", *Experiments in Fluids* Vol. 14, pp. 121-132
- Pallares, J., Cuesta, I., and Grau, F.X., 2002, "Laminar and turbulent Rayleigh-Bénard convection in a perfectly conducting cubical cavity", *International Journal of Heat and Fluid Flow* Vol. 23, pp. 346-358

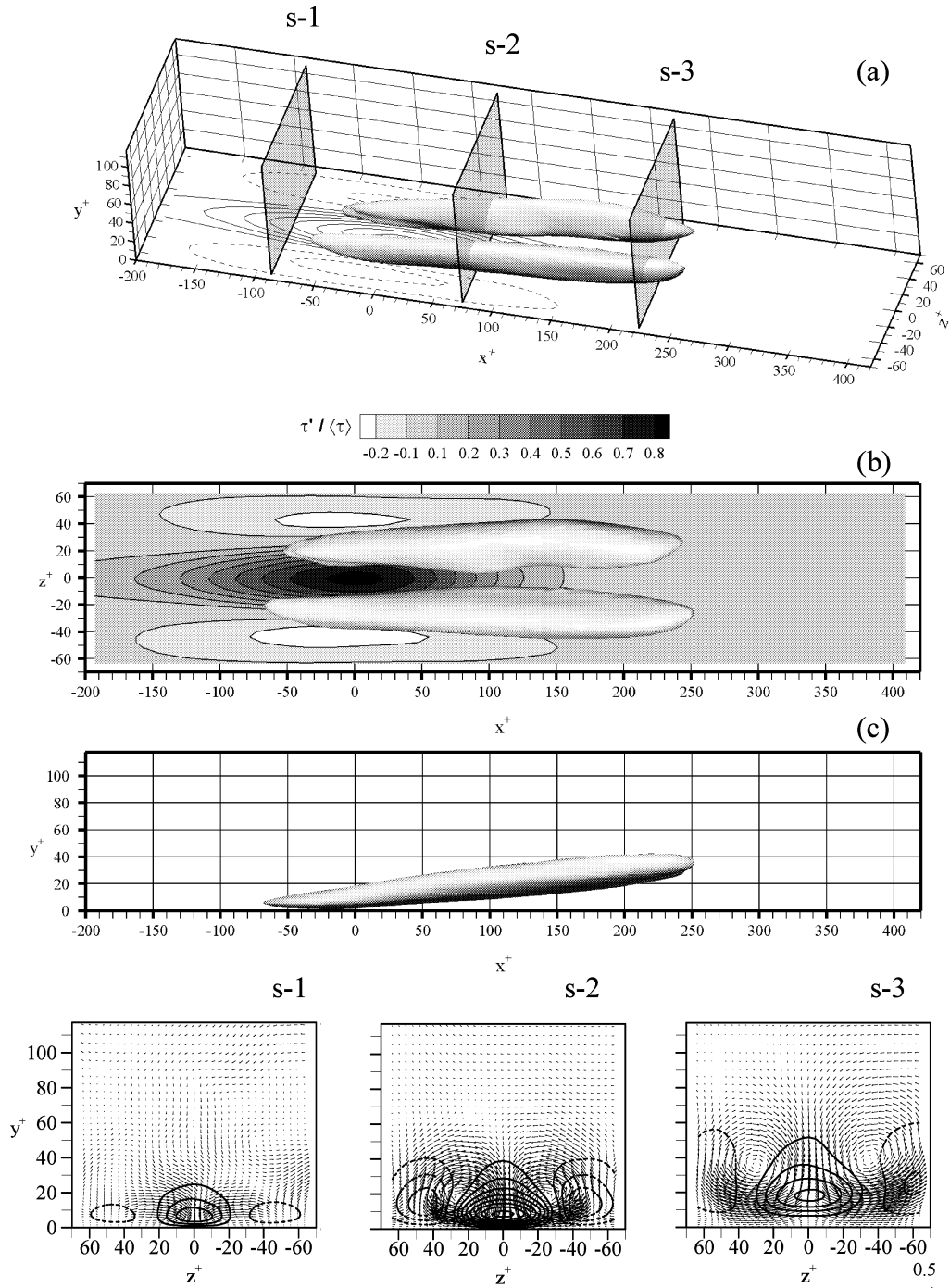


Figure 4. Conditional sampled average flow structure producing a large positive fluctuation of the wall shear stress in terms of the isosurface $\lambda_2 / \text{Max}(\lambda_2) = -0.01$. (a) 3D view (b) top view and (c) side view. The contours at the wall shown in (a) correspond to those depicted in (b). The crossstream fluctuating velocity vector field in the slices indicated in (a) are shown in (s-1) to (s-3). The positive/negative streamwise velocity component is indicated with continuous/dashed line contours. Note that the overall computational domain has dimensions $L_x^+ = 1890$, $L_y^+ = 300$, $L_z^+ = 465$